Thermal activation of photoinduced defects in an intermediate strength quasi-one-dimensional charge density wave solid: PtBr*

Robert J. Donohoe**,[a], C. Anthony Arrington[b] and Basil I. Swanson**,[a]
[a]*Inorganic and Structural Chemistry Group, INC-4, MS-C346, Los Alamos National Laboratory, Los Alamos, NM 87545 (USA)*
[b]*Department of Chemistry, Furman University, Greenville, SC 29613 (USA)*

Abstract

Photoinduced defects in the intermediate strength charge density wave bromide-bridged platinum linear chain (PtBr) have been examined by resonance Raman and electron paramagnetic resonance spectroscopies. A photogenerated signal is observed by the former technique at 130 cm^{-1} and by the latter at $g=2.3$. However, the observed diminishments in these signal intensities upon warming reveal that the Raman feature is not associated with a paramagnetic site. The loss of the 130 cm^{-1} peak upon warming and its nearly complete recovery upon recooling suggest the presence of defect interconversion, possibly an electron bipolaron/polaron equilibrium, while the behavior of the EPR signal upon warming suggests the presence of a range of pinning potentials that lead to distributed kinetic behavior for activation of the paramagnetic sites. The number of defects is dependent upon the phase in which the PtBr sample were crystallized, with the crystals originating in the higher temperature orthorhombic phase supporting greater levels and varieties of defects than those grown in the monoclinic phase.

Introduction

The quasi-one-dimensional inorganic charge density wave (CDW) solids, typified by the halide-bridged platinum group metal (MX) linear chains, are remarkable materials on several counts. First, these materials form highly crystalline anisotropic solids [1] that yield structural information [2] and characterization of the ground and defect states of the CDW by oriented spectroscopic studies. Secondly, the low dimensionality provides for somewhat more tractable theoretical characterization [3], and elaborate models have been developed for the treatment of the electron–electron and electron–phonon forces that dictate the strength of the CDW [4]. Thirdly, the rich history of chemical and physical manipulations of the MX solids has revealed extensive tunability of the strength of the metal sublattice charge disproportionation that characterizes the CDW phase. Although the MX chains have not been

*Invited paper.
**Authors to whom correspondence should be addressed.

0379-6779/92/$5.00

employed for practical applications, the potential utility of low-dimensional materials in sensors, energy storage devices and nonlinear optical devices is now being investigated.

Many research groups, including our own, have concentrated on the characterization of the solids $[M^{II}(L)_2][M^{IV}(L)_2X_2](A)_4$, M = Pt, Pd or Ni, X = Cl, Br or I, L is a bidentate diamine and A is a monoanion. These MX solids define an arena within which the CDW phase adopts a wide variety of strengths and, at least in the case of NiBr [5], can be quenched in favor of a spin density wave. This tunability can be examined with the following diagram:

	Pt	Pd	Ni
Cl	CDW(s)	CDW	?
Br	CDW	CDW(w)	SDW
I	CDW(w)	unk	unk

In this 'periodic chart' of the MX chains, s = strong, w = weak, SDW = spin density wave and unk indicates that the synthesis has not yet been reported. For NiCl, the ground state may depend upon the method of synthesis [6]. Thus, the strength of the CDW is increased as the chart is traversed upwards and to the left. The trend to the left is readily rationalized as a result of decreased electron–electron interactions due to increased shielding while the explanation of the trend upwards is more complex.

A number of studies of MX chains have focused upon PtCl (L = $N_2C_2H_8$), which manifests a strong CDW. In particular, the dimerization of the chloride sublattice (the Peierls distortion) is extreme and the ratio of the short to long Pt–Cl bonds is approximately 3/4 [2a]. In addition, the intervalence charge transfer (IVCT) absorption edge, which is a measure of the gap associated with the charge disproportionation on the metal sublattice, is found near 2.4 eV [7]. As a result of these studies, the spectroscopic properties of the ground state and photogenerated defects have been characterized. Our attention has now been directed toward the bromide analog (PtBr) in order to ascertain the effects of weakening the CDW on the physical properties of this solid. In addition, the recent discovery in our laboratory that PtBr synthesized by the traditional method yields extensive substitution of chloride at the bridging position has elucidated the source of some of the extraordinarily complex data reported for 'PtBr' in the past [8]. At the same time, it has become clear that these mixed halide solid solutions yield spectroscopic behavior much more elaborate than a weighted composite of the signals from the individual pure materials. Several intriguing results derived from mixed halide samples indicate that the interface between different CDW phases leads to unique edge states and stabilized electron/hole separation [9]. In this manuscript, however, we concentrate on the properties of the pure PtBr material. We report some of the spectroscopic signals we have

observed for the ground state and photogenerated defects in PtBr samples that are free of chloride substitution.

Experimental

The PtBr solid was synthesized by the method developed by Huckett *et al.* [8] and judged to be less than 1% contaminated by chloride at the bridging position, as indicated by NMR and Raman measurements. Crystals were grown both above the monoclinic–orthorhombic phase change (PtBr(O), $T_{cryst} = 40$ °C) and below (PtBr(M), $T_{cryst} = 5$ °C). Unless otherwise indicated, spectroscopic measurements were made at a nominal sample temperature of 15 ± 4 K. The Raman instrumentation is described elsewhere. The EPR data were collected with an IBM Instruments Model ER-200 X-band EPR spectrometer with 20 mW power and 20 G modulation amplitude. Crystals were oriented perpendicular to the magnetic field.

Results and discussion

The IVCT absorption edge energy for PtBr has not yet been correctly reported. This is probably due to the fact that most samples have been grown in a contaminated form. In the chloride-free samples, we have observed an intervalence charge transfer band edge near 1.5 eV. However, Kurita has acquired data which suggest that the edge is closer to 1.4 eV [10]. This discrepancy may be due to the manner in which the crystals are grown: the crystals from Kurita's group appear to contain fewer defects and the IVCT edge near 1.4 eV may be more representative of the pure PtBr lattice. In any case, the location of the edge is clearly indicative of a much weaker CDW than is present in PtCl.

Our spectroscopic measurements were made at low temperatures, where both PtBr(O) and PtBr(M) samples are in the monoclinic phase [11]. Thus, PtBr(O) must undergo a phase transition that is quite extensive in terms of unit cell rearrangement. This disruptive transition is known to be first order on the basis of crystallography and calorimetry. Such a transformation might be expected to generate a number of defects that are not observed in the PtBr(M) samples. Direct evidence for this is provided by comparison of the Raman data acquired with excitations below the IVCT edge. Figure 1 compares the Raman data for samples of PtBr(O) and PtBr(M) as acquired with minimum exposure of the crystals to ambient light. Both data sets were obtained for single crystals that were mounted in the cryostat and allowed to sit at room temperature with complete exclusion of light for several days. Apart from the intense ν_1 band (166 cm^{-1}) and a weak peak near 95 cm^{-1}, both of which are associated with the unperturbed PtBr lattice, the PtBr(M) sample reveals only weak intensity for a broad peak near 130 cm^{-1} that is associated with defects. On the other hand, the PtBr(O) sample clearly indicates the

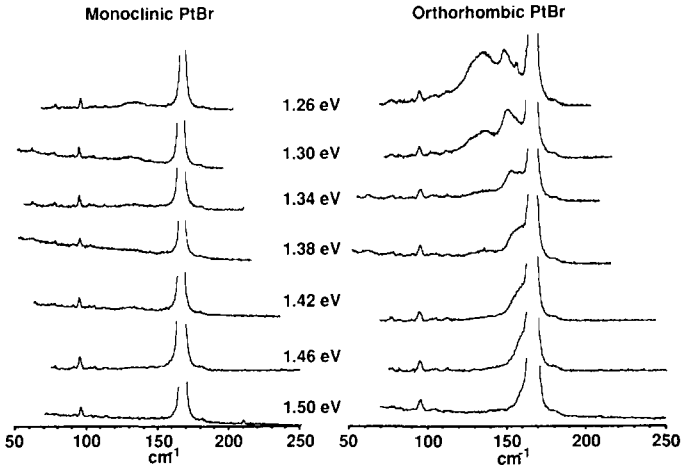

Fig. 1. Resonance Raman data for monoclinic and orthorhombic PtBr at 15 K as a function of excitation energy prior to photolysis. The ν_1 mode (166 cm^{-1}) is off scale in order to emphasize the defect Raman intensities.

presence of a variety of excitation-dependent features upon excitation below the IVCT. In particular, an unresolved peak near 160 cm^{-1} is observed with excitation near the band edge, a peak near 155 cm^{-1} with excitations below 1.4 eV, and both a 150 cm^{-1} peak and a broad band at 130 cm^{-1} as the excitation energy is tuned toward the red limit of our detection system. Clearly, the PtBr(O) sample supports a variety of defects that are not observed in the material which has not undergone the 30 °C phase change. However, these defects are strictly associated with the materials *grown* in the orthorhombic phase. Upon warming a sample of PtBr(M) into the orthorhombic phase (sample was heated to 40 °C) for 2 h and recooling for Raman measurements at low temperature, the 160–150 modes are not in evidence. This suggests a form of crystalline 'memory' in which the defects created upon the orthorhombic to monoclinic phase transition (cooling) are dependant upon the form in which the material was crystallized.

Photolysis of PtCl chains at low temperatures with excitations above the bandgap has been demonstrated to yield metastable defect states [7]. Although the identification of such defects is a subject of debate [12], we concur with the opinion of Kurita that, in PtCl, these defects are hole and electron polarons that are generated from the initial charge transfer state and, upon separation, are either self trapped or pinned by external potential traps. The resonance Raman and theoretical investigations of these defects suggest that electron and hole polarons are each responsible for two electronic transitions immediately below the IVCT edge [4h, 13] (a third band in the mid-infrared is also both predicted by theory and experimentally observed [14]). Lattice dynamics studies of polaron defects are quite successful in reproducing the observed vibrational energies associated with these sites [15]. Electron paramagnetic resonance (EPR) studies of the photolyzed

crystals are consistent with the presence of unpaired spins in the photogenerated defects [7], although the platinum hyperfine pattern is not easily rationalized for polarons [12].

Because a wealth of information has been derived from photolysis studies of PtCl, we have investigated the undoped PtBr crystals under similar conditions. The Raman data of PtBr(M) samples with excitation at 1.26 eV before and after photolysis with 1.65 eV radiation are displayed in the bottom two spectra in Fig. 2. A very broad feature at 130 cm^{-1} gains intensity upon photolysis as well as a weak peak at 90 cm^{-1}. A similar increase is observed in the 130 cm^{-1} band in the PtBr(O) samples, but not in the other defect peaks (150–160 cm^{-1}). The increase in the relative intensity of the 130 cm^{-1} defect mode as the excitation is tuned toward 1.2 eV suggests that the defect absorption band maximum is found in this vicinity. Absorption studies of photolyzed PtBr samples are consistent with this conclusion [16]. In addition, the EPR data reveal an increase in the paramagnetic content of both PtBr(O) and PtBr(M) samples upon photolysis [16]. Although this appears to suggest that the 130 cm^{-1} Raman signal is associated with the paramagnetic defect, we find that this is not the case.

The photoinduced defects in PtBr appear to be metastable at low temperatures. One of the primary motivations for studying the PtBr systems is to examine the kinetics of defect activation by way of comparison with

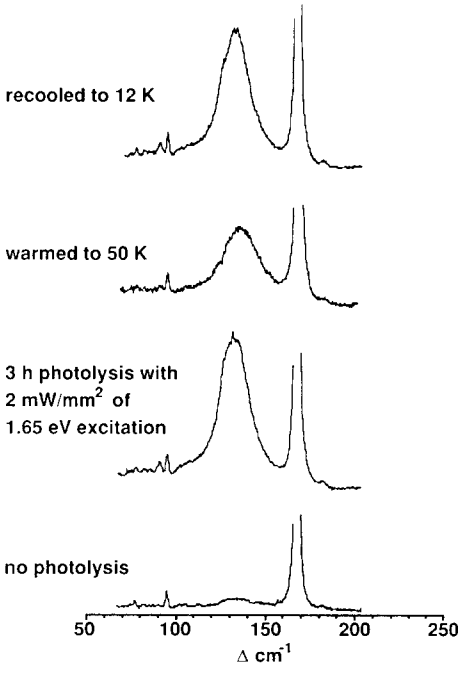

Fig. 2. Resonance Raman spectra of monoclinic PtBr with 1.26 eV excitation as a function of photolysis and then temperature.

the strong CDW system PtCl. As shown in Fig. 2, upon warming of the photolyzed PtBr(M) samples from 12 to 50 K, we observe a dramatic decrease in the 130 cm^{-1} defect peak intensity (there is also a slight increase in the peak energy). However, upon recooling to 12 K, this 130 cm^{-1} peak is largely recovered. Therefore, warming either leads to conversion between defect types (conversion back to the ground state would not lead to recovery of the defect signal upon recooling) or mobilizes the defects so that their electronic and vibrational properties are altered. At 50 K, this is not a complete process as witnessed by the remaining defect vibrational signal.

The photoinduced EPR signal reveals behavior quite distinct from the Raman defect intensity upon warming. Of course, the signal intensity is not only dependent upon concentration but also upon relaxation factors. The EPR signal cannot be observed at 50 K. However, upon warming to 60 K and recooling, the EPR signal is irrevocably reduced by an amount much greater than is observed in the Raman signal. The effects of warming to higher temperatures and recooling will be detailed presently, but warming to 200 K and recooling leads to complete loss of the EPR signal while approximately 50% of the Raman signal is lost. Therefore, the 130 cm^{-1} peak is not associated with the paramagnetic signal.

The activation of defects upon warming can be monitored by EPR despite the loss of signal at elevated temperatures. In Fig. 3, the photoinduced signal observed in a sample of PtBr(M) at 15 K after warming to various temperatures

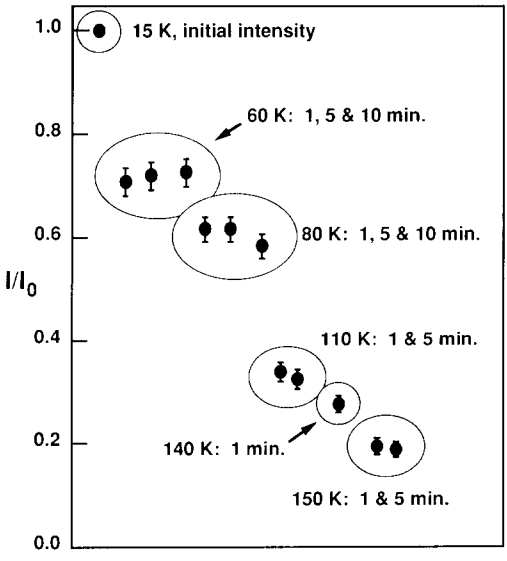

Fig. 3. Comparison of the integrated photoinduced EPR intensity for monoclinic PtBr as measured at 15 K after warming to the indicated temperatures for the indicated lengths of time.

for the indicated lengths of time is divided by the original photogenerated signal intensity. The signal loss upon warming to 60 K for 1 min and recooling is illustrated. Interestingly, rewarming the sample to 60 K for 5 min and recooling does not result in further signal loss. Indeed, within experimental error, the observed signal intensity after warming to 60 K for an additional 10 min and recooling is not altered. On the other hand, warming to 80 K for 1 min and recooling does lead to further signal reduction while, again, rewarming to 80 K for extended periods and recooling does not lead to a similar intensity loss. This effect continues through warming to higher and higher temperatures until all of the signal is gone. These data clearly reveal that the process by which the defects are activated and, eventually, reconverted to the normal chain is mediated by pinning potentials that adopt a variety of magnitudes. Thus, upon warming to 60 K, weakly pinned defects are activated and annihilated while more extensive warming is required to free the more deeply trapped defects. This effect is almost certainly indicative of potential traps due to structural defects, rather than self trapping, although both may occur. Possibly, the range of pinning energies may be due to the distance between a self-trapped defect and a structural defect, with those defects immediately in the vicinity of such a trap strongly pinned. In any case, a simple comparison of defect activation based on the strength of the ground state CDW for PtCl and PtBr is not appropriate.

Two additional issues will now be discussed. First, what information is available on the size (length) of the photoinduced defects? Secondly, what is the nature of the thermally activated defect: is it simply a mobilized form of a formerly trapped defect or is there a temperature-dependent defect interconversion? With regard to the former question, the experimental indication is that the paramagnetic defect is quite extensive, possibly dispersed over more than 10 platinum sites. The evidence for such a description is limited to one PtBr(M) sample which yielded hyperfine structure on the photoinduced EPR signal. This sample may have been a crystal of unusual quality; typically, PtBr crystals are easily fractured and do not archive well. The origin of the hyperfine pattern is not clear. Kawamori *et al.* attributed the narrow hyperfine structure in their data derived from PtCl to spin polarization effects on the amine nitrogens [17]. However, the issue is far from settled, as the expected structure from the bridging chlorine was not in evidence and the assignment of the fine structure to the nitrogens may have been in error. We are currently investigating this by use of ^{15}N-labeled ethylenediamine. In any case, the fine structure on the signal in the PtBr(M) sample is abundant and supports the spatially disperse picture of the paramagnetic defect as a distribution over multiple sites that could reasonably generate such a pattern either due to nitrogens or bromines. It should be noted that, with input parameters partly derived from our experimental results, the two-band model developed by Saxena and Bishop predicts that valence defects such as polarons should be spread over approximately 10 contiguous platinum sites [18]. The spatially disperse view is also consistent with the activation of defects at low temperatures. If their size is not reduced due

to localized trapping sites, the valence defects should be relatively light and easily mobilized.

With regard to the possibility of defect interconversion, the apparent loss of the 130 cm^{-1} peak upon warming in the PtBr(M) samples is not accompanied by an increase in or the advent of another defect Raman mode. However, this is not the case for samples of PtBr(O). As shown in Fig. 4, warming of PtBr(O) samples also causes a reduction in the photoinduced 130 cm^{-1} peak. At the same time, there is a concomitant increase in the 150 cm^{-1} peak. This appears to be a direct indication of defect interconversion in PtBr, but this observation is limited to the orthorhombic form. Furthermore, this interconversion to the defect responsible for the 150 cm^{-1} peak is not completely reversible. This conclusion is not based on careful studies of the temperature dependence of the 130 and 150 cm^{-1} peak intensities upon temperature recycling, but rather on the observation that samples of PtBr(O) that have been photolyzed, warmed to room temperature and then recooled reveal elevated levels of the 150 cm^{-1} peak intensity relative to both ν_1 and the 130 cm^{-1} peak [16]. Apparently, the 150 cm^{-1} defect is due to a structural defect unique to the orthorhombic crystals which traps either a mobilized form of the defect responsible for the 130 cm^{-1} peak or converts that defect into a different defect that is deeply trapped. The latter possibility is consistent with some tentative assignments for the defect modes, which we now discuss.

Because we do not associate the 130 cm^{-1} peak with a paramagnetic defect, we attribute this signal to condensation of two electron polarons into a diamagnetic electron bipolaron. This idea is based in part upon a prediction from lattice dynamics calculations that suggests that 130 cm^{-1} is a reasonable energy for the vibration of such a defect *were it confined to a single platinum site*. Such confinement could occur if a structural trapping site leads to a localized distortion of the lattice, which may in turn lead to heterogeneous broadening of the signal, as appears to be the case with the 130 cm^{-1} mode. Interestingly, the lattice dynamics calculations further suggest that 150 cm^{-1} is the expected energy for a Raman-active mode of localized electron polarons. Therefore, the conversion of the defects associated with 130 cm^{-1} into defects responsible for the 150 cm^{-1} peak may be a result

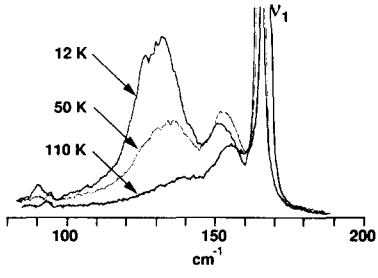

Fig. 4. Temperature dependence of the Raman data for a photolyzed sample of orthorhombic PtBr with 1.26 eV excitation.

of 'melting' of electron bipolarons into polarons. For PtBr, then, photolysis leads to the creation of electron bipolarons and hole polarons, with the latter responsible for the EPR signal. Although calculations have not been attempted for a defect delocalized over multiple sites, we expect that a diffuse defect such as has been indicated by the EPR data will have vibrational energies that are difficult to distinguish from the normal chain. By this effect, the Raman-active modes of a hole polaron may not be readily detected. However, the assignments proposed above will require further testing. In particular, questions to be addressed include: (1) why does the 130 cm^{-1} signal persist longer than the EPR signal? If they are due to distinct photogenerated electron and hole defects, then the simple expectation is that they should be simultaneously annihilated. Does the observation that they are not indicate that hole bipolarons are also formed upon photolysis? (2) Why is the 130 cm^{-1} defect mode so broad? Is this a heterogeneous effect? (3) What is the nature of the unique structural defects in samples of PtBr(O)? Are these associated with broken chains?

Conclusions

The nature of the defects in PtBr is dependent upon sample history, with crystals grown in the orthorhombic phase prone to greater variety and more strongly pinned defects. Photoinduced defects in both PtBr(M) and PtBr(O) samples yield very broad Raman signals at 130 cm^{-1}, with the monoclinic samples essentially defect-free prior to photolysis while the orthorhombic samples retain defects even at room temperature. A photogenerated EPR signal is also observed, although the temperature dependences of the Raman and EPR signals are different. The activation of defects is mediated by pinning potentials in addition to any self trapping and these potentials appear to adopt a variety of magnitudes. Therefore, the strength of the CDW is not the sole determining factor in the kinetic behavior of defects. Defect interconversion may be occurring, and the data are consistent with the possibility of electron bipolaron 'melting' into electron polarons.

Acknowledgements

We gratefully acknowledge Professor Susumu Kurita of the Laboratory of Applied Physics, Faculty of Engineering, Yokohama National University, and Drs Avadh Saxena and Alan Bishop of the Condensed Matter and Statistical Physics Group, T-11, Los Alamos National Laboratory, for making their results available to us prior to publication. This work is supported by the Office of Basic Energy Sciences and the Center for Materials Science at Los Alamos National Laboratory.

References

1 F. Basolo, J. C. Bailar, Jr. and B. R. Tarr, *J. Am. Chem. Soc.*, *72* (1950) 2433.

2 (a) N. Matsumoto, M. Yamashita, I. Ueda and S. Kida, *Mem. Fac. Sci., Kyushu Univ., Ser. C, 11* (1978) 209; (b) H. J. Keller, R. Martin and U. Traeger, *Z. Naturforsch., Teil B, 33* (1978) 1263.; (c) N. Matsumoto, M. Yamashita, S. Kida and I. Ueda, *Acta Crystallogr., Sect. B, 35* (1979) 1458; (d) H. Endres, H. J. Keller, R. Martin, H. N. Gung and U. Traeger, *Acta Crystallogr., Sect. B, 35* (1979) 1885; (e) H. Endres, H. J. Keller, R. Martin, U. Traeger and M. Novotny, *Acta Crystallogr., Sect. B, 35* (1980) 35; (f) H. J. Keller, B. Müller, G. Ledezma and R. Martin, *Acta Crystallogr., Sect. C, 41* (1985) 16; (g) M. Yamashita, K. Toriumi and T. Ito, *Acta Crystallogr., Sect. C, 41* (1985) 876.

3 M.-H. Whangbo, *Acc. Chem. Res.*, *16* (1983) 95.

4 (a) K. Nasu, *J. Phys. Soc. Jpn.*, *52* (1983) 3865; (b) K. Nasu and A. Mishima, *Rev. Solid State Sci.*, *2* (1988) 539; (c) D. Baeriswyl and A. R. Bishop, *J. Phys. C: Solid State Phys.*, *21* (1988) 339; (d) A. Mishima and K. Nasu, *Phys. Rev. B, 39* (1989) 5758; (e) S. D. Conradson, M. A. Stroud, M. H. Zietlow, B. I. Swanson, D. Baeriswyl and A. R. Bishop, *Solid State Commun.*, *65* (1988) 723; (f) A. Mishima and K. Nasu, *Phys. Rev. B.*, *39* (1989) 5763; (g) A. R. Bishop, J. T. Gammel and S. R. Phillpot, *Synth. Met.*, *29* (1989) F151; (h) J. T. Gammel, R. J. Donohoe, A. R. Bishop and B. I. Swanson, *Phys. Rev. B, 42* (1991) 10 556; (i) A. R. Bishop, *Synth. Met.*, in press.

5 K. Toriumi, Y. Wada, T. Mitani, S. Bandow, M. Yamashita and Y. Fujii, *J. Am. Chem. Soc.*, *111* (1989) 2341.

6 D. A. Cooper, S. J. Higgins and W. Levason, *J. Chem. Soc. Dalton Trans.*, (1983) 2131.

7 S. Kurita and M. Haruki, *Synth. Met.*, *29* (1989) F129.

8 S. C. Huckett, R. J. Donohoe, L. A. Worl, A. D. F. Bulou, C. J. Burns, J. R. Laia, D. Carroll and B. I. Swanson, *Chem. Mater.*, *3* (1991) 123.

9 L. A. Worl, A. Saxena, A. R. Bishop and B. I. Swanson, manuscript in preparation.

10 S. Kurita, personal communication.

11 Neutron diffraction data for both forms of PtBr at 11 K indicate that no phase changes occur below 30 °C: S. C. Huckett, unpublished data.

12 N. Kuroda, M. Sakai, M. Suezawa, Y. Nishina and K. Sumino, *J. Phys. Soc. Jpn.*, *59* (1990) 3049.

13 R. J. Donohoe, C. D. Tait and B. I. Swanson, *Chem. Mater.*, *2* (1990) 315.

14 R. J. Donohoe, S. A. Ekberg, C. D. Tait and B. I. Swanson, *Solid State Commun.*, *71* (1989) 49.

15 A. D. F. Bulou, R. J. Donohoe and B. I. Swanson, *J. Phys. C: Solid State Phys.*, in press.

16 R. J. Donohoe, L. A. Worl, C. A. Arrington, A. D. F. Bulou and B. I. Swanson, *Phys. Rev. B.*, submitted for publication.

17 A. Kawamori, R. Aoki and M. Yamashita, *J. Phys. C: Solid State Phys.*, *18* (1985) 5487.

18 A. Saxena and A. R. Bishop, manuscript in preparation.